DRC-1007

Trajectory Tracking Control of a Magnetic Wheel Wall Climbing Robot

Eiammanussakul T. and Sangveraphunsiri V.*

Department of Mechanical Engineering, Faculty of Engineering, Chulalongkorn University
Phya Thai Road, Khwaeng Wangmai, Khet Pathumwan, Bangkok, 10330
*Corresponding Author Email: Viboon.S@eng.chula.ac.th, Tel: 0-2218-6610-1, Fax: 0-2252-8889

Abstract

A wall climbing robot using magnetic wheels is used for inspection of weld beads on large steel tanks. The research work purposes a high precision trajectory tracking controller for a magnetic wheel mobile robot. Nonlinear tracking control laws were designed regarding a nonholonomic constraint and a kinematic model of the mobile robot so that the convergence of errors in position and orientation was guaranteed. Multiple sensors were utilized to obtain accurate location of the robot and to improve control loop performance. Experimental results showed that with the tracking controller the robot could track the predefined straight trajectory, as in the real application, with maximum errors of 1 millimeter in position and 0.01 radian in orientation although imperfections of dimensions of driving mechanism and from the environment might be existed.

Keywords*:* wall climbing robot, trajectory tracking, multiple-sensor localization

1. Introduction

A wall climbing robot using magnetic wheels is proposed in a large tank inspection process instead of scaffolding. The benefits of using the robot are reachability in hazardous areas, cheaper and less time-consuming compared to scaffolding [1]. In addition, the robot's ability to locate itself in the inspection path and even to mark damaged areas [2] could facilitate the maintenance services.

The main application of this robot is the inspection of weld beads on a large steel tank. These weld beads were usually aligned in straight lines joining pieces of steel plates together to form a large tank. In this case, the robot paths for the inspection task are straight lines which could be predefined before the operation.

Some concerning issues in the process involve a tracking control problem and localization of the robot. Controlling the robot is not simple because the robot is subjected to a nonholonomic constraint [8] that does not allow the robot the move in lateral direction. The control algorithm must be designed regarding the constraint in order to successfully navigate the robot along the desired path. Moreover, the kinematic model of the robot is nonlinear so the stability of the control variables must be determined.

Position estimation is another challenging problem. The position and orientation of the robot

must be precisely acquired in order to navigate the robot to the correct location [3], [4]. Odometry is a basic position estimation based on wheels' rotation on the robot. However, this approach usually suffers from systematic errors (such as imperfect dimension of driving mechanisms) and non-systematic errors (such as slippage and non-uniform floors) [5]. Many research papers suggest combining information from multiple sensors to obtain the better posture estimation of the robot. These additional sensors are usually exteroceptive sensors such as vision sensors, laser rangefinders, and inertial sensors.

In this study, the tracking control algorithm is designed regarding the nonholonomic constraint and the kinematic model of the mobile robot. The combination of multiple sensors such as wheel encoders and a vision sensor are developed to obtain position and orientation of the robot. Experiments are conducted to demonstrate how the controller could improve the tracking performance of the robot along the predefined straight line trajectory.

2. Wall Climbing Robot

2.1 Structure

The wall climbing robot in Fig. 1 consists of three magnetic wheels aligned in tricycle configuration. Two drive wheels are located at front of the robot with their axes coincident. Each wheel was differentially actuated by a DC motor in the similar way as a differential-drive robot. Motor shafts are connected with harmonic reduction gears to provide enough traction force for propelling the robot on a vertical surface. The other magnetic wheel is located at the back of the robot to

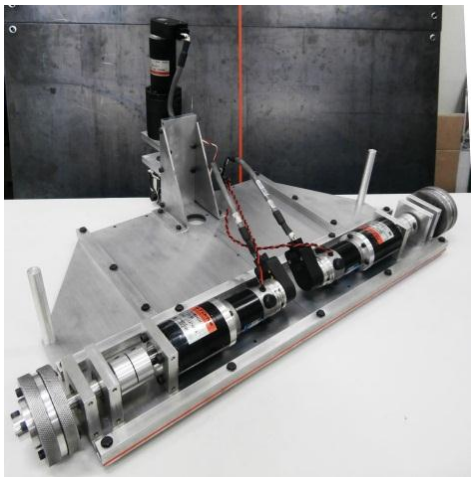

Fig. 1 Magnetic Wall Climbing Robot with Magnetic Wheels

maintain the robot on the planar surface. The rear wheel steers the robot with an angle corresponding to the front wheels' rotation. In order to produce a cooperative movement, every wheel axis intersects at a point, namely, an instantaneous center of rotation.

2.2 Robot Location Representation

The robot location can be defined by two frames represented in Fig. 2. The inertial coordinate (frame I) is fixed at the start point of the robot movement. The other frame is the robot coordinate (frame R) which is located at the center of the robot (point P) on the front wheels axes at distances x and y with respective to the inertial coordinate. The x-axis of the robot coordinate (X_R) points along the heading of the robot. The angle formed by X_R and X_I is the orientation of the robot (θ). Thus, the location of the robot is defined by three variables which are $q = \begin{bmatrix} x & y & \theta \end{bmatrix}^T$.

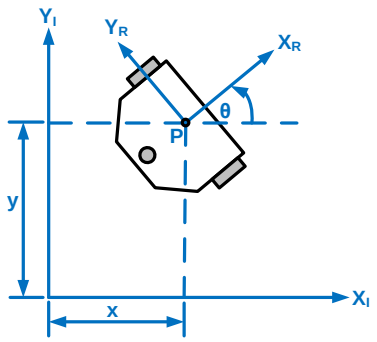

Fig. 2 Coordinates representing the location of the robot

2.3 Wheel Constraint and Kinematic Model

A robot is assumed to move without slipping. This implies that the robot cannot move laterally along its wheel axes. This assumption associates with a nonholonomic constraint described by the following equation.

$$\dot{x}\sin\theta - \dot{y}\cos\theta = 0 \qquad (1)$$

Eq. (1) can be written into multiplying matrices as

$$\begin{bmatrix}\sin\theta & -\cos\theta & 0\end{bmatrix}\begin{bmatrix}\dot{x}\\ \dot{y}\\ \dot{\theta}\end{bmatrix} = 0$$

$$A\dot{q} = 0$$

Kinematic model of the robot is the null space of the constraint matrix (A). This relationship is in differential form (relationship of velocities) which cannot be integrated due to the nonholonomic constraint.

$$\begin{bmatrix}\dot{x}\\ \dot{y}\\ \dot{\theta}\end{bmatrix} = \begin{bmatrix}\cos\theta & 0\\ \sin\theta & 0\\ 0 & 1\end{bmatrix}\begin{bmatrix}v\\ \omega\end{bmatrix} \qquad (2)$$

where v is the heading velocity of the robot (in X_R direction), and ω is the turning velocity of the robot.

A differential-drive robot has forward kinematics representing the relationship between drive wheel rotational velocities and robot velocities as

$$\begin{bmatrix}v\\ \omega\end{bmatrix} = \frac{r}{N}\begin{bmatrix}1/2 & 1/2\\ 1/L & -1/L\end{bmatrix}\begin{bmatrix}\dot{\varphi}_1\\ \dot{\varphi}_2\end{bmatrix} \qquad (3)$$

where $\dot{\varphi}_1$ and $\dot{\varphi}_2$ are rotational velocities of the right and left wheel respectively, r is the drive wheel radius, L is the distance between wheels along their wheel axes, and N is the gear reduction ratio of a harmonic gear.

The conversion of matrix in Eq. (3) called inverse kinematics is described as

$$\begin{bmatrix}\dot{\varphi}_1\\ \dot{\varphi}_2\end{bmatrix} = \frac{N}{r}\begin{bmatrix}1 & L/2\\ 1 & -L/2\end{bmatrix}\begin{bmatrix}v\\ \omega\end{bmatrix} \qquad (4)$$

3. Control System

3.1 Tracking Control

In this research, the robot is given a predefined trajectory. The path is a straight line in vertical orientation with the timing law as s-curve trajectory. The advantage of a s-curve trajectory over a ramp trajectory is the lower acceleration and deceleration which could prevent a robot from slip and reduce tracking errors [6].

In order to obtain the desirable movement of the robot, reference variables that needed to be controlled are then described as follows:

$$\begin{bmatrix} x_r \\ y_r \\ \theta_r \end{bmatrix} = \begin{bmatrix} s-curve\ trajectory \\ 0 \\ 0 \end{bmatrix}$$

Since the x-position reference is selected as a s-curve trajectory, the heading velocity reference (differentiated position reference) is described as a trapezoidal trajectory whereas the turning velocity reference is zero.

$$\begin{bmatrix} v_r \\ \omega_r \end{bmatrix} = \begin{bmatrix} trapezoidal\ trajectory \\ 0 \end{bmatrix}$$

Position and orientation errors are computed into tracking errors as

$$\begin{bmatrix} x_e \\ y_e \\ \theta_e \end{bmatrix} = \begin{bmatrix} \cos\theta & \sin\theta & 0 \\ -\sin\theta & \cos\theta & 0 \\ 0 & 0 & 1 \end{bmatrix} \begin{bmatrix} x_r - x \\ y_r - y \\ \theta_r - \theta \end{bmatrix}$$

By differentiating these errors and modifying the equation by Eq. (2), the error dynamics is derived.

$$\begin{bmatrix} \dot{x}_e \\ \dot{y}_e \\ \dot{\theta}_e \end{bmatrix} = \begin{bmatrix} v_r \cos\theta_e \\ v_r \sin\theta_e \\ \omega_r \end{bmatrix} + \begin{bmatrix} -1 & y_e \\ 0 & -x_e \\ 0 & -1 \end{bmatrix} \begin{bmatrix} v \\ \omega \end{bmatrix} \quad (5)$$

The error dynamics is used to compute the new desired velocities $\dot{q}_d = [v_d \quad \omega_d]$ for the robot to navigate itself back to the path. By considering Lyapunov function proposed by [7], the desired velocities are derived.

$$V = \frac{1}{2}\left(x_e^2 + y_e^2\right) + \frac{1-\cos\theta_e}{k_y}$$

where k_y is a gain controlling the robot to move in y-direction.

By differentiating the Lyapunov function and substituting with Eq. (5):

$$\dot{V} = x_e\left(v_r \cos\theta_e - v + y_e\omega\right) + \ldots$$
$$+ y_e\left(v_r \sin\theta_e - x_e\omega\right) + \left(\omega_r - \omega\right)\sin\theta_e$$

$$\dot{V} = \left(v_r \cos\theta_e - v\right)x_e + \sin\theta_e\left(v_r y_e + \omega_r - \omega\right) \quad (6)$$

Desired heading and turning velocities of the robot $(v_d,\ \omega_d)$ are selected.

$$v = v_d = v_r \cos\theta_e + k_x x_e \quad (7)$$

$$\omega = \omega_d = \omega_r + v_r k_y y_e + k_\theta \sin\theta_e \quad (8)$$

where k_x is a gain controlling the robot to move in x-direction and k_θ is a gain controlling the orientation of the robot.

By substituting of equation (7) and (8) into equation (6),

$$\dot{V} = -k_x x_e^2 - \frac{k_\theta \mathrm{v}_r \sin^2\theta_e}{k_y}$$

It can be observed that the differentiated Lyapunov function is always less than zero ($\dot{V}$ is negative definite) as x_e and v_r are not zero in the same time. Therefore, with the heading velocity reference pointing forward $(v_r \geq 0)$ and choices of control gains $k_x,\ k_\theta \geq 0$ and $k_y > 0$ the convergence of position and orientation errors are guaranteed.

3.2 Localization

In this research, localization of the robot is based on information from two sensors, namely, wheel encoders and a camera. This combination could give a better position estimation of the robot by proper selection from their advantages. Position and orientation of the robot in each control loop sampling can be estimated from odometry which is computed from wheel encoder rotation by kinematics in Eq.(1) and Eq.(3). However, this approach works well in a short period of time (and a short path) because the inaccuracy of robot dimension and wheel slip produce small amount of position errors which could grow significantly over time [9].

Another information source of robot location is from visual sensing. A monocular camera is placed perpendicular to the test surface at a fixed distance. Although the camera could give a global position of the robot in the platform regardless on systematic and non-systematic errors, the control loop usually suffers from its slow update rate. Image acquiring and processing could slow the control loop down to only 4 Hertz sampling rate. Furthermore, discontinuity of robot position directly affects the performance and stability of the control system [10].

To obtain better position estimation, the image acquiring and processing loop which is operating at slow sampling rate is separated from the control loop which maintains its high sampling rate for good control performance. The location of the robot is based on vision sensor when the camera received new information and is estimated by odometry during the information from the camera is not updated.

3.3 Control Block Diagram

The overall control of the robot represented in Fig. 3 consists of two levels. The outer loop compares estimated location from odometry and a camera with the reference positions and orientation. The errors and reference velocities are inputted into the tracking control to calculate the desired velocities needed to navigate the robot back to the reference trajectory. Desired wheel rotation velocities are then computed by inverse kinematics in Eq. (4) and pass into the motor control loop (the inner loop). Angular positions of each drive motor are then controlled with PID controllers.

4. Experiment

The wall climbing robot was tested to verify the effectiveness of the derived tracking control. The test platform in Fig. 4 was 70-degree inclined flat steel plates with 4-millimeter thickness along with a camera located a meter away from the platform to cover the entire view. The image acquiring and processing loop and tracking control loop are implemented on LabVIEW based on a host PC computer. Control signal and power are transmitted to the robot through umbilical cables for fast communication (compared to wireless communication) and weight reduction of the robot (no additional batteries on the robot).

The reference path of the robot was a 1.2-meter long straight line pointing upwards. The maximum reference velocity and acceleration of the robot were selected at 50 mm/s and 50 mm/s^2 respectively so that a slow speed movement of the robot in real inspection processes is imitated.

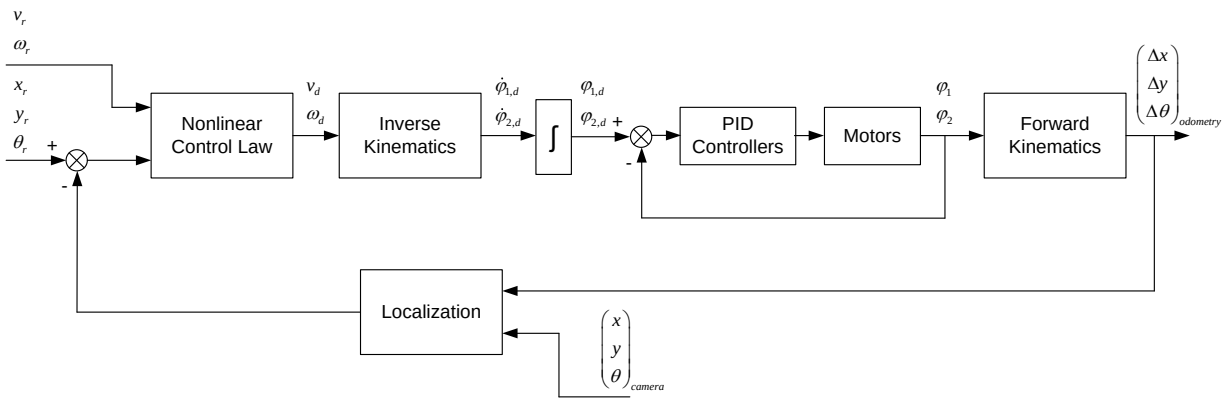

Fig. 3 Tracking Control Block Diagram

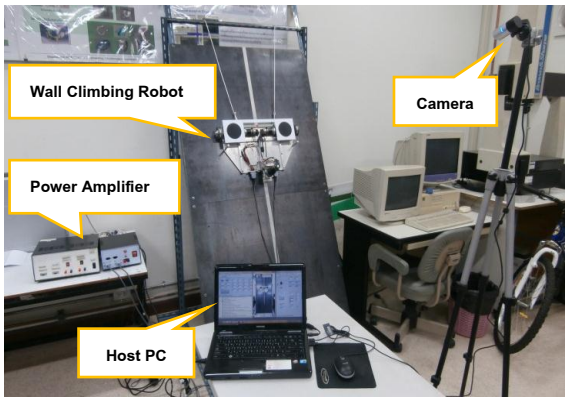

Fig. 4 Experiment Rig

The experiment was divided into two sections. Firstly, the robot was assigned to move along the trajectory without the tracking control by feeding reference velocities directly into the motor control loop. In the next section, the robot was controlled by the tracking controller. The position and orientation of the robot from these two sections were compared to analyze the performance of the tracking control algorithm.

5. Result and Discussion

The position and orientation of the robot when moved along a predefined straight trajectory without and with tracking control are illustrated in Fig. 5.

In Fig. 5(c), without the tracking controller, the robot turned right (positive value) immediately at the start of the move. The angle gradually grew larger at a very slow rate throughout the rest of the move. This caused the robot to move out of the straight path as shown in Fig. 5(b). Even though the distance deviated from the path at the end of the move was only 4.5 millimeters to the right, it can be seen that the robot was not tend to be back in the path again. This implies that the robot might deviate to a significant distance if the robot operates on the longer path.

The movement behavior of the robot without tracking control was clearly influenced by errors from many sources. Firstly, acceleration of the robot might be too high so the robot slipped and deviated from the path at the start of the move. In addition, the imperfect dimension of wheels and driving mechanism might cause the robot to turn away from the path gradually throughout the rest of the move.

With the tracking control whose gains were selected as $k_x = 0$, $k_y = 1000$ and $k_\theta = 8$, the robot had the better movement. According to Fig. 5(b) and 5(c), the robot moved with maximum deviation of 1 millimeter and orientation of 0.01

radian. Although imperfection of the robot's dimension and wheel slippage might be existed, these errors did not tend to diverge. Therefore, it might be concluded that the proposed control algorithm could navigate the robot along a predefined trajectory with small errors and might be applicable to a longer distance, for example, in a tank inspection.

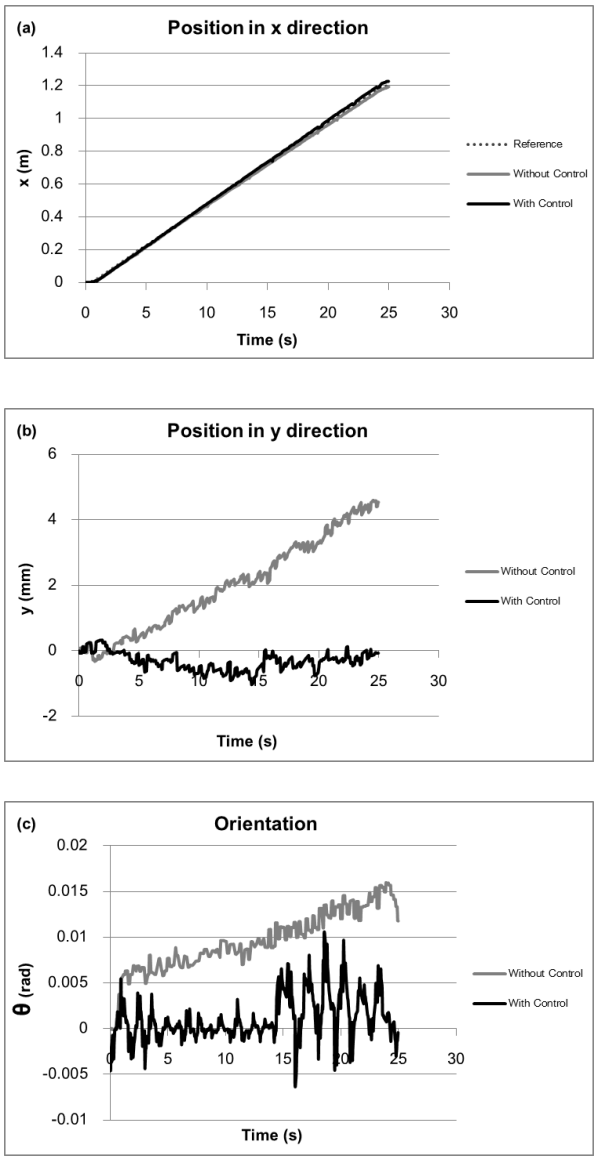

Fig. 5 Position and Orientation of the robot

(a) position in x direction

(b) position in y direction

(c) orientation

6. Conclusion

This paper presents the tracking control of the magnetic wheel wall climbing robot regarding the nonholonomic constraint and kinematic model. The combination of information from wheel encoders and a vision sensor is used to obtain better estimation of robot position and orientation. The experiment results showed that the proposed tracking control and localization technique can improve the tracking performance of the robot.

7. Future Work

In this study, the robot was assigned to move along a predefined straight trajectory. However, in a practical situation the robot has to track along weld beads on a large steel tank which may not be aligned perfectly straight. Therefore, the path generation of the robot should be further developed based on the real environment during the process. One possible idea is to mount a camera on the robot to localize weld beads and construct new position and orientation reference to the robot.

8. Acknowledgement

This work is sponsored by the Regional Center of Robotics Technology and the Chulalongkorn University under Chulalongkorn University Centenary Academic Development Project.

9. Reference

9.1 Proceedings

[1] Fernández, R., González, E., Feliú, V, and Rodríguez, A.G. (2010). A Wall Climbing Robot for Tank Inspection for Tank Inspection. An

Autonomous Prototype, paper presented in the 36th Annual Conference on IEEE Industrial Electronics Society, Arizona, USA.

[2] Fondahl, K., Eich, M., Wollenberg, J., Kirchner, F. (2012). A Magnetic Wall Climbing Robot for Marine Inspection Services, paper presented in the 11th International Conference on Computer and IT Applications in the Maritime Industries, Liège, Belgium.

[3] Yap, T. Jr., Li, M., Mourikis, A. I., and Shelton, A. R. (2011). A Particle Filter for Monocular Vision-Aided Odometry, paper presented in the IEEE International Conference on Robotics and Automation 2011, Shanghai, China.

[4] Goncalves, J., Lima, J., nad Costa. P. (2008). Real-time localization of an omnidirectional mobile robot resorting to odometry and global vision data fusion: an EKF approach, paper presented in the IEEE International Symposium on Industrial Electronics 2008, Cambridge, UK.

[5] Borenstein, J. and Feng, L. (1996). Gyrodometry: A New Method for Combining Data from Gyros and Odometry in Mobile Robots, paper presented in the IEEE International Conference on Robotics and Automation 1996, Minnesota, USA.

[6] Nandy, S., Shome, S. N., Somani, R., Chakraboty, G., and Kumar, C. S. (2011). Detailed Slip Dynamics for Nonholonomic Mobile Robotic System, paper presented in the IEEE International Conference on Mechatronics and Automation 2011, Beijing, China.

[7] Gholipour, A. and Yazdanpanah, M. J. (2003). Dynamic Tracking Control of Nonholonomic Mobile Robot with Model Reference Adaptation for Uncertain Parameters, paper presented in the 38th European Control Conference, Cambridge, U.K.

9.2 Books

[8] Siegwart, R. and Nourbakhsh, I. R. (2004). Introduction to Autonomous Mobile Robots, the MIT Press, London.

[9] Siciliano, B., Sciavicco, L., Villani, L., and Oriolo, G. (2009). Robotics Modelling, Planning and Control, Springer, London.

[10] Sangveraphunsiri V. (2004). Control of Dynamic Systems, Chulalongkorn University Press, Bangkok.